



9-2016

Capture and Recycle of Industrial CO₂ Emissions Using Mircoalgae

Michael H. Wilson

University of Kentucky, michael.wilson@uky.edu

Daniel T. Mohler

University of Kentucky, daniel.mohler@uky.edu

John G. Groppo

University of Kentucky, john.groppo@uky.edu

Thomas E. Grubbs

University of Kentucky, thomas.grubbs@uky.edu


Stephanie Kesner

University of Kentucky, stephanie.kesner@uky.edu

See next page for additional authors

Right click to open a feedback form in a new tab to let us know how this document benefits you.

Follow this and additional works at: https://uknowledge.uky.edu/caer_facpub

 Part of the [Bioresource and Agricultural Engineering Commons](#), [Chemical Engineering Commons](#), [Chemistry Commons](#), and the [Power and Energy Commons](#)

Repository Citation

Wilson, Michael H.; Mohler, Daniel T.; Groppo, John G.; Grubbs, Thomas E.; Kesner, Stephanie; Frazar, E. Molly; Shea, Aubrey; Crofcheck, Czarena L.; and Crocker, Mark, "Capture and Recycle of Industrial CO₂ Emissions Using Mircoalgae" (2016). *Center for Applied Energy Research Faculty Publications*. 8.
https://uknowledge.uky.edu/caer_facpub/8

Authors

Michael H. Wilson, Daniel T. Mohler, John G. Groppo, Thomas E. Grubbs, Stephanie Kesner, E. Molly Frazar, Aubrey Shea, Czarena L. Crofcheck, and Mark Crocker

Capture and Recycle of Industrial CO₂ Emissions Using Microalgae**Notes/Citation Information**

Published in *Applied Petrochemical Research*, v. 6, issue 3, p. 279-293.

© The Author(s) 2016

This article is distributed under the terms of the Creative Commons Attribution 4.0 International License (<http://creativecommons.org/licenses/by/4.0/>), which permits unrestricted use, distribution, and reproduction in any medium, provided you give appropriate credit to the original author(s) and the source, provide a link to the Creative Commons license, and indicate if changes were made.

Digital Object Identifier (DOI)

<https://doi.org/10.1007/s13203-016-0162-1>

Capture and recycle of industrial CO₂ emissions using microalgae

Michael H. Wilson¹ · Daniel T. Mohler¹ · John G. Groppo¹ · Thomas Grubbs¹ ·
Stephanie Kesner¹ · E. Molly Frazar¹ · Aubrey Shea² · Czarena Crofcheck² ·
Mark Crocker^{1,3}

Received: 8 January 2016 / Accepted: 3 June 2016 / Published online: 16 June 2016
© The Author(s) 2016. This article is published with open access at Springerlink.com

Abstract A novel cyclic flow photobioreactor (PBR) for the capture and recycle of CO₂ using microalgae was designed and deployed at a coal-fired power plant (Duke Energy's East Bend Station). The PBR was operated continuously during the period May–September 2015, during which algae productivity of typically 0.1–0.2 g/(L day) was obtained. Maximum CO₂ capture efficiency was achieved during peak sunlight hours, the largest recorded CO₂ emission reduction corresponding to a value of 81 % (using a sparge time of 5 s/min). On average, CO₂ capture efficiency during daylight hours was 44 %. The PBR at East Bend Station also served as a secondary scrubber for NO_x and SO_x, removing on average 41.5 % of the NO_x and 100 % of the SO_x from the flue gas. The effect of solar availability and self-shading on a rudimentary digital model of the cyclic flow PBR was examined using Autodesk Ecotect Analysis software. Initial results suggest that this is a promising tool for the optimization of PBR layout with respect to the utilization of available solar radiation.

Keywords Algae · Carbon dioxide · Photobioreactor · Flue gas · Power plant · Utilization

Paper for submission to Applied Petrochemical Research (5th KOPRC Forum Special Publication: “The Continuing Role of Fossil Fuels in the Transformation to a Sustainable Energy Future”).

✉ Mark Crocker
mark.crocker@uky.edu

¹ Center for Applied Energy Research, University of Kentucky, Lexington, KY 40511, USA

² Department of Biosystems and Agricultural Engineering, University of Kentucky, Lexington, KY 40506, USA

³ Department of Chemistry, University of Kentucky, Lexington, KY 40506, USA

Introduction

Fossil fuels, including coal, will remain the main source of electric power for at least several more decades. Hence, there is a need for technologies to curb CO₂ emissions to the atmosphere to allow the use of these fuels in more carbon neutral ways. One approach involves CO₂ capture and long-term storage underground. However, current technologies for CO₂ recovery and compression are energy intensive; indeed, system analyses suggest that their use would typically impose a parasitic plant load in the range of 30–35 % [1]. Consequently, there is interest in exploring other approaches to CO₂ mitigation, among which the use of microalgae to biologically capture and recycle CO₂ appears promising. In this approach, there is the potential to obtain valuable biomass-derived products which can help to offset the costs of CO₂ capture.

The concept of using microalgae to mitigate CO₂ emissions from industrial point sources is not new [2–5]. To this end, a number of studies have been performed to determine the ability of microalgae to withstand the high CO₂ concentrations present in flue gas [6–9] as well as the potentially toxic accompanying SO_x and NO_x gases [10–12], and screening studies have been conducted to identify algae species that are particularly suited for this type of application [13–15]. A limited number of proof-of-concept studies have also been performed using flue gas from combustion sources such as stationary engines and, in some cases, power plants [5, 16]. However, to date there have been few published studies concerning large-scale demonstrations of CO₂ capture from flue gas by algae, although one company, Seabiotic, has utilized flue gas from a coal burning power station for algae cultivation. Flue gas from Israel Electric Corporation's Ashkelon power station was fed to algae ponds, the produced algae

being sold as a food additive [17]. In addition, several demonstrations are in progress at power plants in such geographically diverse regions as Australia, Germany, China, Taiwan, South Africa and the USA [5].

We have previously reported the results of studies conducted at a coal-fired power plant (Duke Energy's East Bend Station, located in Boone County, KY, USA) [18]. Initial evaluations led to the conclusion that algae cultivation sized to reduce the CO₂ output of a power plant would need to be of an enormous scale. Photobioreactors (PBRs) were, therefore, chosen as the cultivation system of choice on the basis of their higher areal productivities [19], as well as potential for higher CO₂ capture efficiencies and limited water loss due to evaporation [20]. Subsequently, a vertical tube PBR was designed, prototyped and refined, with emphasis placed on cost minimization [18]. Indeed, capital costs are critical because of the scale inherent in trying to capture large quantities of CO₂. In tandem, a low-cost growth medium for algae cultivation was devised, based on ingredients available on the agricultural commodity market [21], and an inexpensive process for algae harvesting and dewatering was implemented based on sequential flocculation, sedimentation and gravity filtration [18, 22]. These innovations culminated in the deployment of a pilot-scale (18,000 L) demonstration facility at East Bend Station, which was commissioned in December 2012. Using a strain of *Scenedesmus* native to Kentucky (*Scenedesmus acutus*, UTEX B72), algae productivity of routinely ≥ 30 g/(m² day) was achieved in the summer months, while average daily productivity slightly in excess of 10 g/(m² day) was demonstrated in the month of December.

Based on the data collected at East Bend, a techno-economic analysis indicated that from a process perspective the largest sources of cost reside in the algae culturing stage, corresponding mainly to the capital cost of the photobioreactor system and the associated installation [18]. Subsequent work has, therefore, focused on the implementation of cost reduction measures to the PBR, resulting in a radically new PBR design. In this contribution, we present the main features of this cultivation system, together with basic data characterizing the system performance. Ongoing efforts to further improve system productivity are also highlighted.

Experimental

Scenedesmus acutus was obtained from the University of Texas Culture Collection (UTEX B72). A urea medium previously optimized for this *Scenedesmus* strain [21] was used for all experiments. Cultures were initially grown in Erlenmeyer flasks (500 mL) under warm (Philips F32T8/

TL741 Alto, 32 W) and cool white (Philips F32T8/TL735 Alto, 32 W) fluorescent lights [70 $\mu\text{mol}/(\text{m}^2 \text{ s})$] in a 16:8 h light:dark illumination period. Flasks were bubbled with 3 % CO₂ (balance N₂) at room temperature (22 °C). The cultures were subsequently transferred to 7.5 L airlift photobioreactors (PBRs) located in a greenhouse and supplied with 3 % CO₂ and natural light. A number of airlift PBRs were used to seed a 1200 L cyclic flow PBR at East Bend Station. The latter was constantly monitored by probes for pH (Hach PC1R2A), dO₂ (Hach 5740DOB), reactor and ambient temperature (J thermocouples) and photosynthetically active radiation (PAR, Apogee Instruments SQ-215). Temperature, PAR, dissolved O₂, and pH signals were measured using national instruments (NI) cRIO CPU modules and interpreted by NI Labview software. The composition (O₂, CO₂, NO_x and SO_x concentrations) and temperature of the inlet flue gas and outlet PBR exhaust gas were also monitored and recorded (MRU Instruments Vario Plus Industrial Flue Gas Analyzer). These data were logged by their respective analyzers and were later correlated with the other data logged using NI Labview software.

Culture growth at East Bend Station was monitored by means of dry mass (g/L) [21] and qualitative microscopy analyses. Additionally, ultraviolet–visible spectrophotometry (Thermo Scientific Evolution 60) was used to monitor the density of algal cultures, absorbance being measured at 680 nm. Typically, three 50 mL samples were taken daily from the PBR for analysis. The concentrations of urea and specific nutrient ions were tracked to determine the rate of nutrient consumption. Anion and cation concentrations in the cyclic flow reactor were monitored by ion chromatography (IC, Dionex ICS 1100). Samples for urea analysis were run on a Dionex Ultimate 3000 Standard Liquid Chromatography System. The urea analysis method utilized a Thermo Acclaim mixed-mode HILIC-1 analytical column with a mobile phase of 30 % acetonitrile in water, a flowrate of 1.0 mL/min at ambient temperature, UV detection at 200 nm and a sample run time of 9 min.

Results and discussion

Cyclic flow photobioreactor development

In our previous publication, the development of a continuously circulating closed-loop PBR was described [18]. As a result of operating experience gained in the field, the PBR was extensively redesigned, resulting in the next generation 'cyclic flow' PBR used in the present study. The redesigned PBR consists of clear vertical tubes (to maximize sunlight exposure), each of which is sparged periodically with flue gas. The tubes are filled with the algae culture by

means of a pump, although the pump is not operated continuously; rather, it is used to periodically fill and drain the tubes. In this manner, pumping energy requirements are significantly reduced over conventional PBR systems (vide infra).

The PBR body consists of a system of vertical tubes made of clear PET (polyethylene terephthalate) tubes (8.9 cm diameter \times 244 cm high) connected by 7.5 cm diameter schedule 40 PVC (polyvinyl chloride) pipe. To increase individual tube access to solar radiation and minimize shading, reactor tubes are arranged in two parallel manifold lines offset, so that each tube is centered between the empty spaces of the other (Fig. 1). Figure 2 depicts a computer-generated image of the PBR tube arrangement along with a photograph of an installed pilot-scale system.

The ‘cyclic flow’ reactor is designed to operate very differently than other PBR designs. In addition to the high energy penalty associated with the continuous circulation of large volumes of algae culture, unintended consequences can arise. Fully developed flow in a pipe results in a ‘no slip’ condition at the pipe wall. This provides convenient conditions for algae cells to accumulate on the wall of the tube. Given time, these cells will colonize and form a biofilm; indeed, biofilm formation has been a major technical hurdle to the deployment and scale up of photobioreactors. To avoid this issue, the culture in the new reactor does not flow continuously. Instead, the tubes in the photo array drain and fill in a cyclic manner multiple times per day. Consequently, the liquid flow is never fully developed and biofilm formation is minimized. In the cyclic flow PBR, biofilm mitigation is additionally controlled by the introduction of gas bubbles in the PET tubes to create multi-dimensional fluid mixing, and through the use of a buoyant pipe pig (one per PET tube) to clean the reactor walls as flow is cycled. Each time the reactor is filled and drained the pipe pigs—which are equipped with rubber gaskets—travel the length of the clear PET tubes, mechanically removing any attached algae (confirmed by visual inspection).

Instead of sparging gas and/or circulating the culture continuously, energy savings are realized by duty cycling these operations based on the needs of the algae culture for mixing, ensuring suspension of the culture, and providing adequate CO₂. A schematic flow diagram of the system is shown in Fig. 3. A main process tank (1) is sized to be equal to or greater than the volume of one phototube array, consisting of two parallel manifold lines. A centrifugal pump and valving system (2) are used to move algae slurry from the process tank to the phototube arrays (6), from the phototube arrays back to the tank for mixing and/or harvesting (3), and to mix the culture via a recycle line (4). An overflow line (5) enables gas, originally in the empty tubes,

to be transferred to the tank during fill cycles and for the same volume of gas to be transferred back to the phototube array during draining cycles to prevent suction from damaging the semi-rigid PET tubes. Flue gas is periodically added directly to the phototubes via perforated tubing (13) to mix the culture and add CO₂. Algae are harvested via a harvest port (7) and sent to a primary dewatering system to separate the algae from the nutrient medium (8). Clarified water (containing any unused nutrients) is returned (9) to the process tank via a UV sterilizer (10) to prevent contamination of the system. The feed and drain valves (2, 3) are repeated for each additional tube array to accommodate a series of parallel reactors which operate separately. Labview software is used to control the actuation of the process valves, start and stop the pump, actuate solenoid valves to control the injection of flue gas to the system, and monitor process parameters such as photo-synthetically active radiation, pH, dissolved oxygen, and temperature.

Water, a seed culture, and nutrients are added to the main process tank and mixed via a centrifugal pump before the algae slurry is sent to fill the phototube array. This process is repeated until all the phototube arrays are filled for normal operation. The vertical phototubes create a quiescent water column, providing the algae with access to photoactive radiation. The culture is periodically sparged with flue gas to mix the culture, control pH, and provide multidimensional fluid flow to control biofilm. Multiple times per day, the entire volume in the phototube array is drained to disrupt biofilm formation, enable mixing of the culture to maintain homogeneity of the system, and to actuate pipe pigs in each tube. The separate phototube arrays share a main process tank with the periodic draining and mixing set on a predetermined duty cycle.

Photobioreactor energy consumption

As noted above, in previous work a continuously circulating closed-loop PBR was developed and trialed [18]. The resulting cascade in each row of the PBR allowed for an eductor effect, facilitating the injection of flue gas into the reactor without gas compression or sparging. However, the PBR incurred large energy penalties in the form of head losses and high pump duties due to the required flow conditions and continuous liquid movement throughout the system.

To evaluate the energy requirements of the cyclic flow and the continuous flow PBRs, the liquid flowrate, head losses and pump duty were calculated for each system. The flow rate of the PBR was in each case normalized according to the total system volume serviced by the pump and was used, in combination with the calculated head loss, to calculate the energy requirements of circulating the

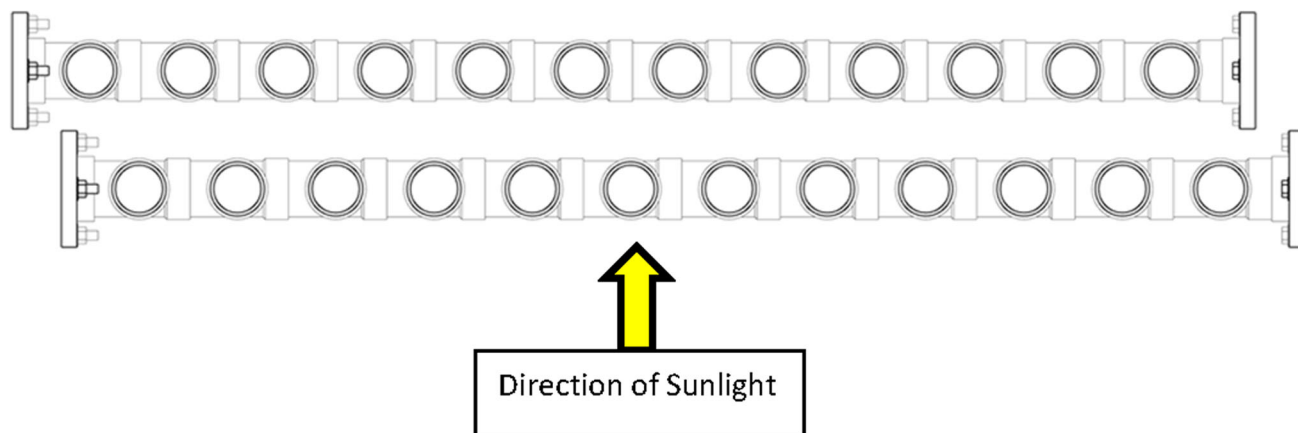
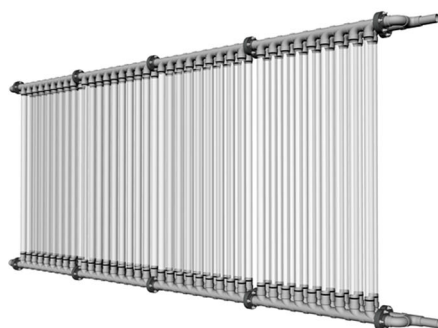


Fig. 1 Overhead view of parallel manifolds showing alignment of tubes to minimize shading

Fig. 2 Computer-generated image showing PBR tube arrangement and photograph of an installed pilot-scale PBR



algae culture. The comparison of the two PBR designs is reported in Table 1. Notably, the pump duty per liter of reactor for the cyclic flow PBR is some three orders of magnitude lower than that of the continuously circulating PBR. The two reactors have very different geometries and flow paths, which in turn affect the friction loss associated with the liquid flow. The continuous flow reactor is composed of tubes connected in parallel by a series of 90° turns, while the cyclic flow PBR consists of multiple parallel flow paths fed from a common manifold. This lower resistance is an important factor in reducing operating costs, but the duty cycle of the pump has an even larger contribution. The continuous flow PBR pump is operated continuously to mix the algae culture (12 h/day with minimal flow at night), requiring a large central process pump, whereas the cyclic flow reactor is designed to periodically (4–6 times per day) drain and fill the tubes to ensure culture homogeneity and to actuate the pipe pigs for biofilm control.

Figure 4 shows the overall comparison between the two PBRs, displaying the total energy requirement for each. The case considered was a hypothetical 1 MW coal-fired

power plant, with CO₂ capture at the 30 % level. Even with the energy requirement for gas compression accounted for (flue gas compression from atmospheric pressure to 1 bar gauge), the total energy requirement of the cyclic flow PBR is only 8 % that of the continuously circulating PBR at the design flow rate. As shown, decreasing the liquid flow rate in the continuous flow PBR helps to decrease the energy consumption; however, even when operating at 50 % of the design flow rate (the lowest realistic flow rate to maintain flue gas eduction), the energy requirement is still significantly greater than the cyclic flow PBR.

Photobioreactor demonstration

Field testing of the cyclic flow photobioreactor was conducted at Duke Power's East Bend Station located in Boone County, Kentucky, USA. This single unit (650 MW) plant burns high sulfur coal as the fuel source and utilizes a wet limestone scrubber for SO_x control and selective catalytic reduction (SCR) with ammonia injection for NO_x control, resulting in low flue gas concentrations of NO_x and SO_x [18]. Flue gas used for algae growth studies

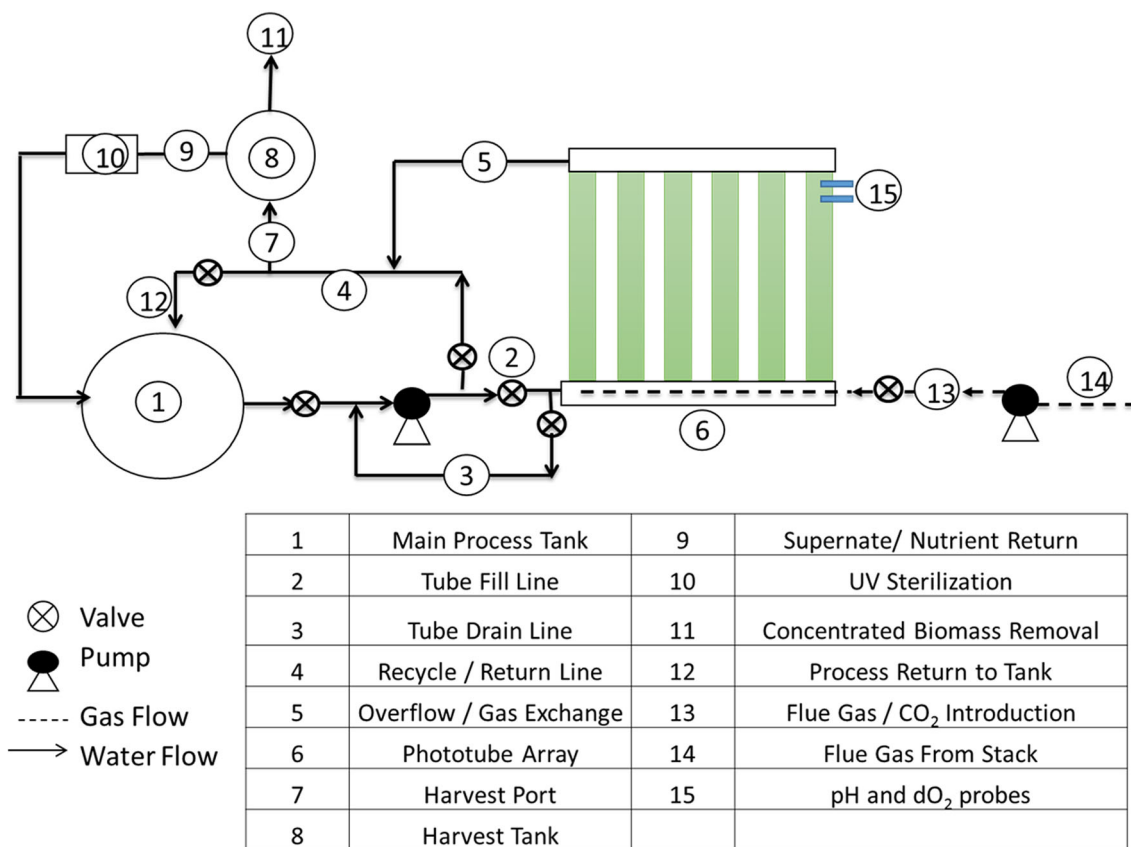


Fig. 3 Process flow diagram of photobioreactor

Table 1 Comparison of cyclic flow and continuous flow photobioreactors

PBR design	Liquid flow rate (Q/V, min ⁻¹)	Head loss (m/L)	Pump duty (W/L)
Cyclic flow	6.94E-03	2.60E-03	3.70E-05
Continuous flow	1.72E-02	2.07E-02	1.90E-02

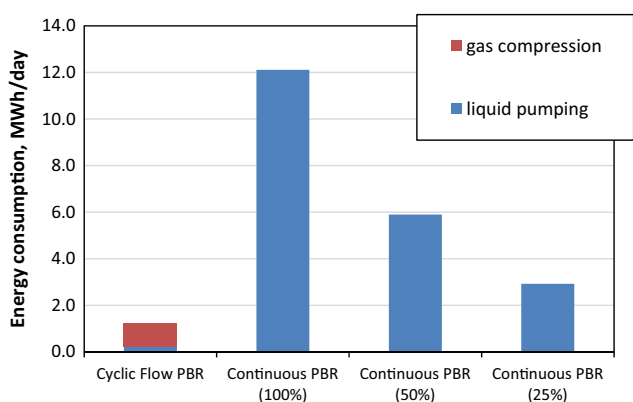
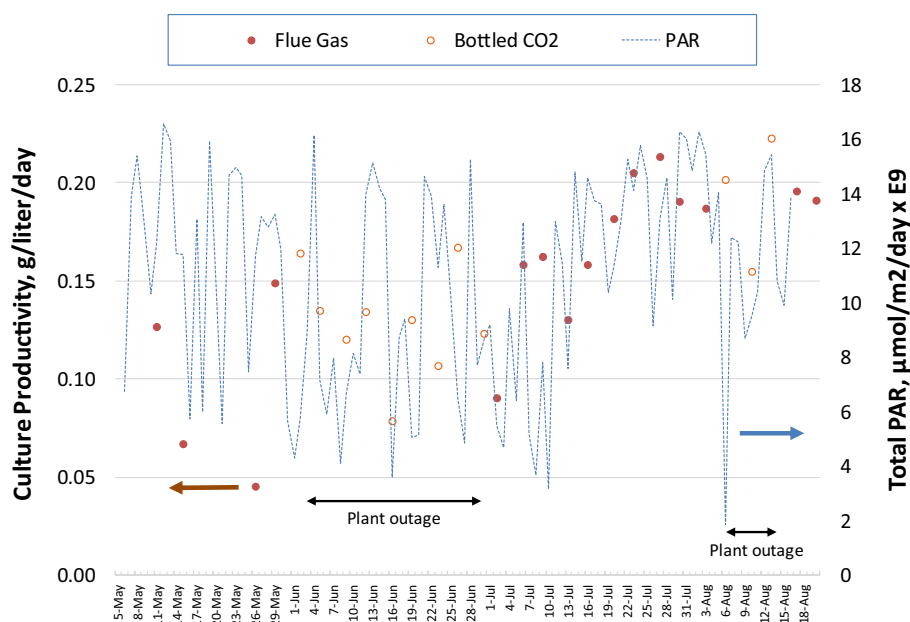


Fig. 4 Comparison of energy consumption for cyclic flow and continuous flow PBRs (1 MW coal-fired power plant, 30 % CO₂ capture). Values for the continuous flow PBR are shown at 100, 50 and 25 % of the design liquid velocity in the PBR

was obtained after the scrubber and SCR unit and was delivered to the site via a 1" stainless steel pipe, driven by a diaphragm vacuum pump. The demonstration site is located on the east side of the power plant and sits on a concrete pad poured above a gravel drainage bed lined with a geomembrane below a French drain to collect all surface run-off and any potential tube leakages. Water used to fill the PBR was drawn from several wells on the property and passed through a UV sterilizer to minimize potential contamination by any organisms present.

The pilot-scale cyclic flow reactor consisted of two sets of 36 tubes comprising parallel rows (offset to allow better access to solar radiation) for a total of 300 gallons (1148 L). The reactor was inoculated on May 6th, and was operated continuously until mid-September. Twice per week, 80 % (240 gallons) of the system was harvested and

Fig. 5 Algae culture productivity and daily integrated PAR vs. time



dewatered using a two-stage dewatering process developed in house [22]. ≥ 95 % of the harvested volume, along with any unused nutrients, was returned to the system as clarified water via a UV sterilizer to control contaminants and predators that may have entered during the dewatering process. Nutrients and make-up water (≤ 5 % system volume) were then added to the reactor to enable continued operation and culture growth. The remaining algae slurry was further dewatered via gravity filtration. Once all the free water was separated from the algal biomass, the samples were dried (48 h at 60 °C), weighed, and stored.

Figure 5 shows the productivity of the cyclic flow reactor at East Bend Station along with daily integrated photosynthetically active radiation (PAR) during the growth campaign. Interruptions in flue gas availability, due to power plant outages or the flue gas pump being out of service, are indicated on the graph by hollow circles. During this time, a gas stream of 10 mol % CO₂ mixed with air was fed to the reactor (using bottled CO₂ and compressed air) to maintain culture health and productivity. As expected, periods of strong algae growth showed a strong correlation with high levels of PAR. As shown in Fig. 5, productivities typically ranged between 0.1 and 0.2 g/(L day), with an average value of 0.165 ± 0.057 g/(L day), representing an improvement over the previous PBR design which showed a mean volumetric growth rate of 0.047 ± 0.042 g/(L day) for the period June–July 2013.

Flue gas uptake

An example of typical inlet flue gas composition is shown in Fig. 6. Off-peak hours are indicated by arrows, during

which a reduction in CO₂ and an increase in O₂ can be observed due to plant ramp down. During off-peak hours, the plant burns less coal, increasing the percentage of residual air in the flue gas. This effect is also shown in Figs. 8 and 9 as a change in the inlet concentrations of CO₂ and O₂.

Typical PBR performance with respect to CO₂ capture is depicted in Fig. 7. On August 30, the culture was harvested, involving the removal of 240 gallons of culture and the addition of an equal volume of clarified water (recycled from the previous harvest) and nutrients. Immediately afterwards, the outlet gas composition of the PBR was monitored. Initially, a large difference between the inlet and outlet CO₂ concentrations was observed (ca. 6 mol.%); this gradually decreased as the make-up water became saturated with CO₂. After ~ 1 h, the outlet CO₂ concentration was stabilized, indicating that the system had reached equilibrium. This was achieved with a sparge (flue gas injection) time of 20 s/min (i.e., 20 s on and 40 s off), resulting in a baseline CO₂ emission reduction of ~ 20 %.

Higher CO₂ capture efficiencies were realized by reducing the length of the sparge time. This is illustrated by the data shown in Figs. 8, 9, and 10, which were obtained with the use of a sparge time of 5 s/min (5 s on and 55 s off). Notably, several correlations are evident from these figures, including the fact that rising PAR values resulted in increased temperatures within the reactor. Moreover, a direct correlation between rising PAR values and the divergence of both inlet and outlet CO₂ and O₂ compositions was observed. Specifically, outlet compositions of CO₂ and O₂ decreased and increased, respectively, with increased sunlight (Figs. 8, 9). This is a direct indication of

Fig. 6 CO₂ and O₂ concentration (mol.%) in flue gas during daytime and nighttime operation vs. time

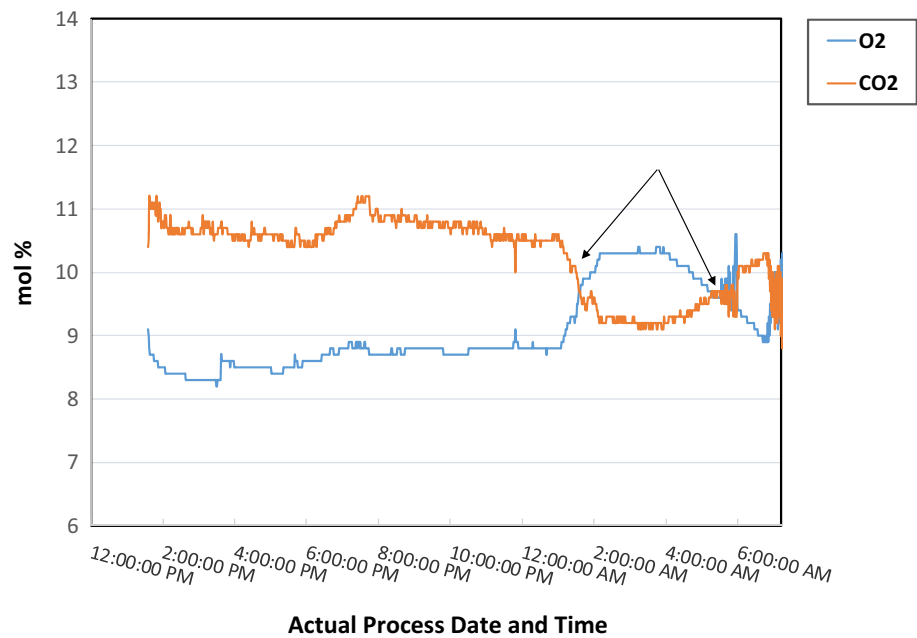
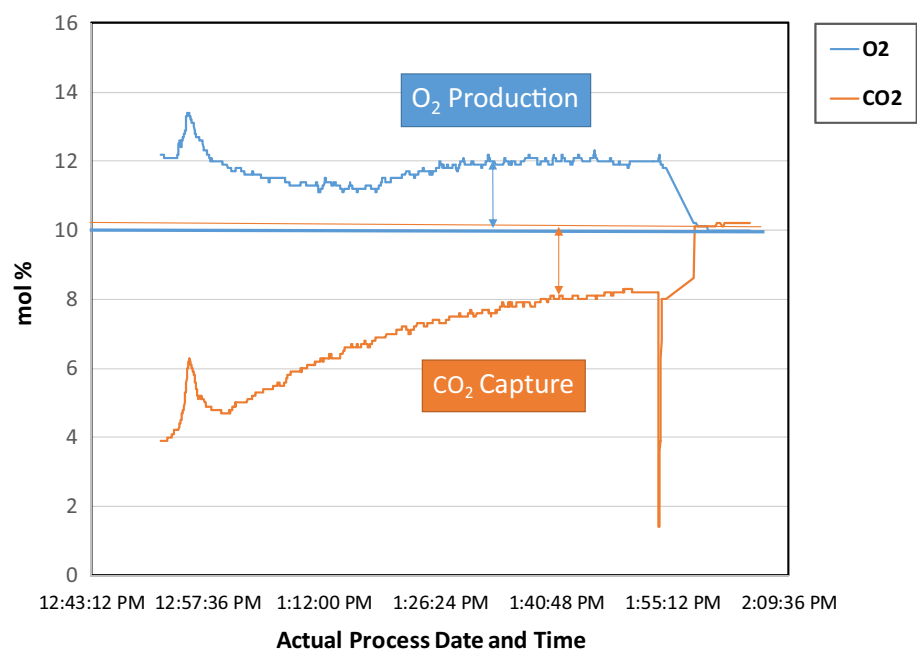


Fig. 7 CO₂ and O₂ concentration (mol.%) at PBR inlet and outlet. Red and blue arrows indicate the difference in inlet and outlet concentrations for both species



O₂ production and CO₂ consumption via photosynthesis, as further evidenced in Fig. 10 which directly compares outlet CO₂ and O₂ concentrations. As shown in Fig. 8, CO₂ capture efficiency peaked during peak sunlight hours, the largest recorded CO₂ emission reduction occurring midday on September 17, corresponding to a value of 81 %. On average, CO₂ capture efficiency during daylight hours (using a 5 s sparge time) was 44 %.

The PBR at East Bend Station also served as a secondary scrubber for NO_x and SO_x, removing on average

41.5 % of the NO_x and 100 % of the SO_x from the flue gas as shown in Figs. 11 and 12. Both Figs. 11 and 12 contain the same temperature data as Figs. 8, 9, and 10, while Fig. 12 also contains the same PAR data. According to Fig. 12, the SO_x concentration in the flue gas at the PBR inlet appears to be correlated with the PAR and reactor temperature, as evidenced by the sinusoidal shape of the plots and the matching wavelength. This phenomenon can be attributed to two factors. First, during off-peak hours, the SO_x (and NO_x) concentration in flue gas decreased due

Fig. 8 CO₂ inlet and outlet concentration (mol.%), temperature inside the reactor (°C) and PAR [$\mu\text{mol}/(\text{m}^2 \text{ s})$] vs. time

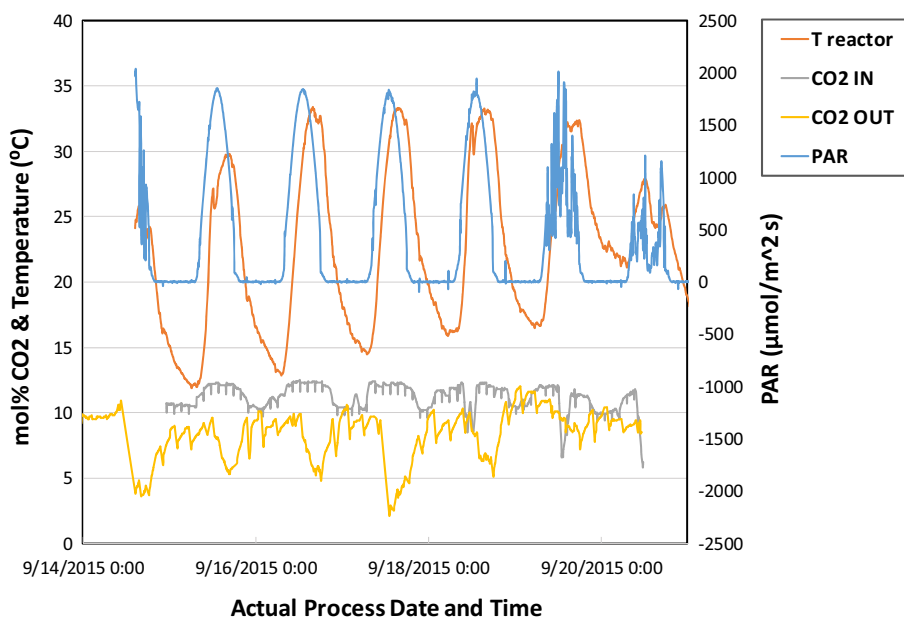
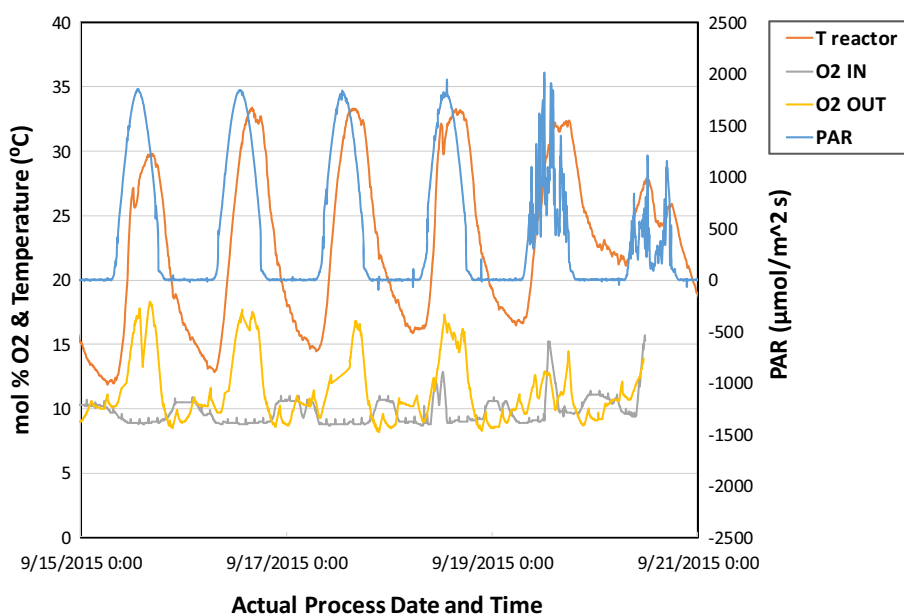


Fig. 9 O₂ inlet and outlet concentration (mol.%), temperature inside the reactor (°C) and PAR [$\mu\text{mol}/(\text{m}^2 \text{ s})$] vs. time



to the plant ramp down. Second, water vapor in the flue gas tended to condense in the line leading to the PBR, the water being removed in a trap upstream of the PBR. As a consequence of the high solubility of SO_x in water (228 g/L at STP [23]), a significant amount of dissolved SO_x was removed from the flue gas with the condensed water, the amount of water removed being greater during the nighttime (off-peak hours) than daytime due to the lower ambient temperature. Of the SO_x that remained in the gas phase (0.61 mg/min on average), 100 % was absorbed by the PBR. Moreover, analysis of sulfate levels in the liquid medium in the PBR (see following section) showed no

accumulation of sulfate during the course of the growing season, indicating that the algae were able to metabolize the relatively small amounts of sulfur introduced into the PBR. However, an important distinction between NO_x and SO_x removal was observed. NO_x mainly consisted of NO which possesses only very low solubility in water (0.098 g/L at STP [24]). Consequently, NO_x removal in the condenser upstream of the PBR was minimal.

It is also noteworthy that NO_x and SO_x removal efficiencies remained roughly constant during both the day and night, each staying within an average range of 35–45 and 100 %, respectively. During nighttime operation, flue gas

Fig. 10 CO₂ and O₂ outlet concentration (mol.%), temperature inside the reactor (°C) and PAR [$\mu\text{mol}/(\text{m}^2 \text{ s})$] vs. time

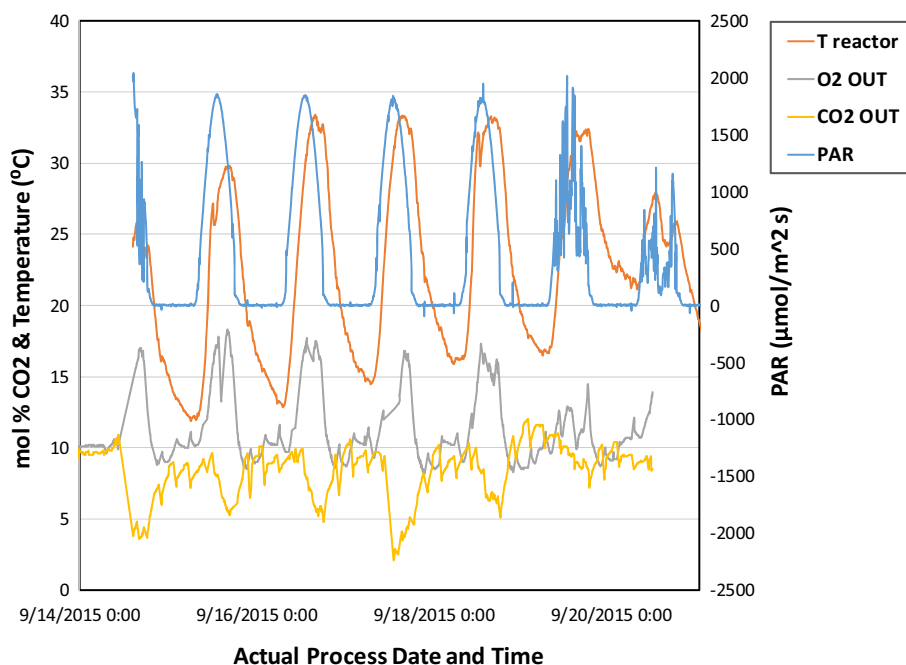
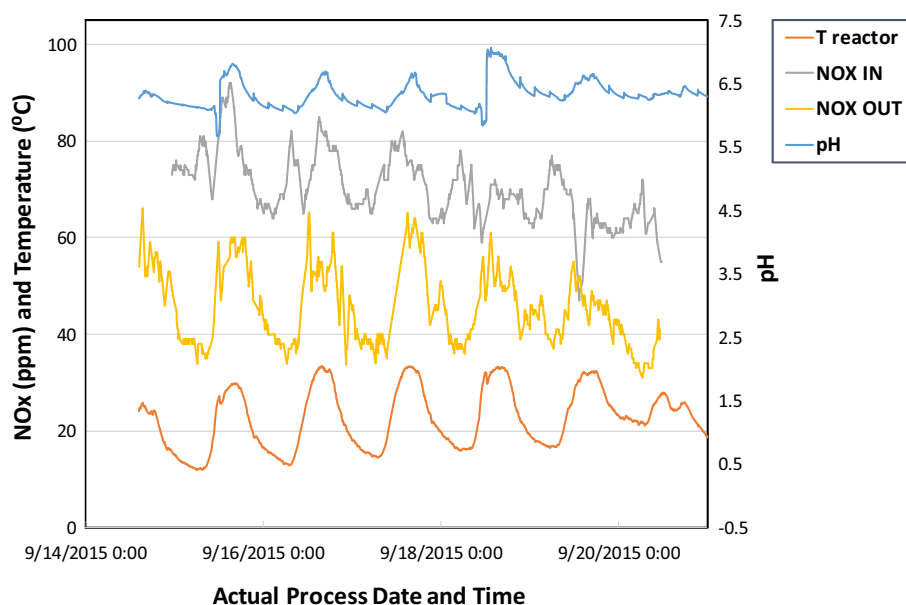


Fig. 11 NO_x inlet and outlet concentration (ppm), temperature inside the reactor (°C) and PAR [$\mu\text{mol}/(\text{m}^2 \text{ s})$] vs. time



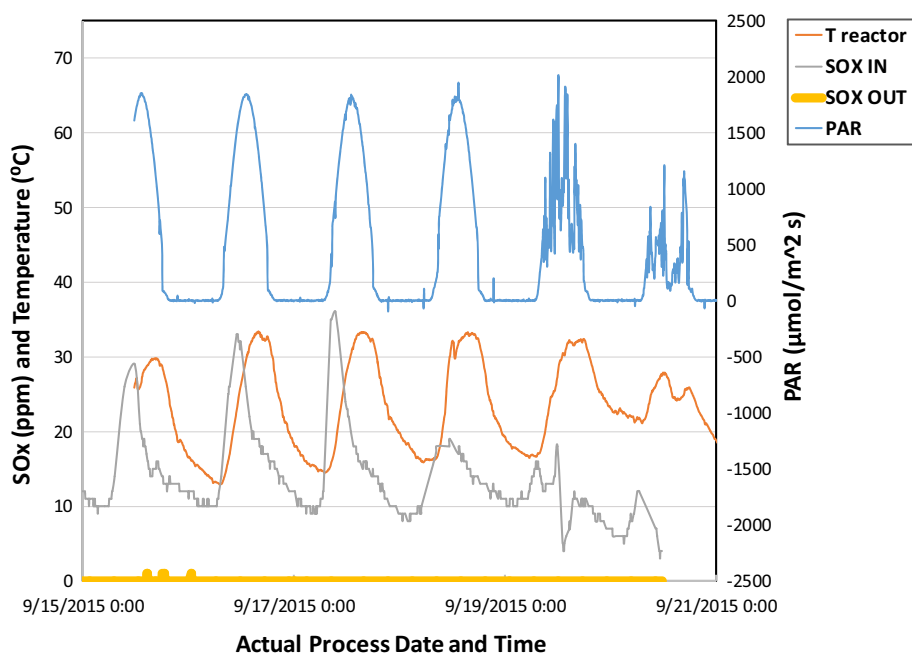
was sparged with the same frequency as during the daytime to ensure that the algae remained in suspension, with no attempt to control the pH. Consequently, in the absence of photosynthesis, the pH of the culture tended to decrease during the night. As shown in Fig. 11, maximum pH values of typically 6.5–6.9 were attained during periods of maximum PAR, when CO₂ capture peaked. During night-time operation, when CO₂, NO_x and SO_x addition continued but without CO₂ capture (and with respiration resulting in slightly elevated levels of CO₂), the pH dropped to values in the range 6.0–6.3. Evidently, self-buffering of the

system prevents pH values from dropping precipitously. This, combined with the exceptional tolerance of this *Scenedesmus* strain for acidic conditions [15], means that high culture productivity can be maintained even in the absence of external pH control.

Nutrient consumption

Nutrient concentrations in the PBR were tracked by means of ion chromatography (ionic species) and HPLC (urea). Figures 13 and 14 collect the data for the cations and

Fig. 12 SO_x inlet and outlet concentration (ppm), temperature inside the reactor (°C) and PAR [$\mu\text{mol}/(\text{m}^2 \text{ s})$] vs. time



anions, respectively, for a 2-month period; for comparison purposes, both figures also contain the corresponding urea data. It should be noted that samples were taken for analysis immediately prior to algae harvesting. Consequently, the urea concentration followed a saw-tooth pattern, consistent with regular urea consumption and nutrient replenishment after each harvest. The amplitude of this pattern remained relatively constant during the months of August and September with a typical decrease in the urea

concentration of 100–150 ppm for each period between harvests. PO_4^{3-} showed a similar yet more inconsistent pattern of consumption during growth cycles.

During the period of August 31 through September 4, the urea concentration decreased while the concentration of NH_4^+ increased, although the consumption patterns remained constant. This drop in urea and rising NH_4^+ concentration can be attributed to an escalation in urea hydrolysis caused by an increase in average reactor

Fig. 13 Concentration of cationic species and urea in the PBR vs. time. *Error bars* represent the standard deviation of single measurements on triplicate samples. Note that the substantial decreases in K^+ concentration on August 10 and September 14 were due to the fact that fresh make-up water was added to the reactor (after algae harvesting) instead of recycled growth medium

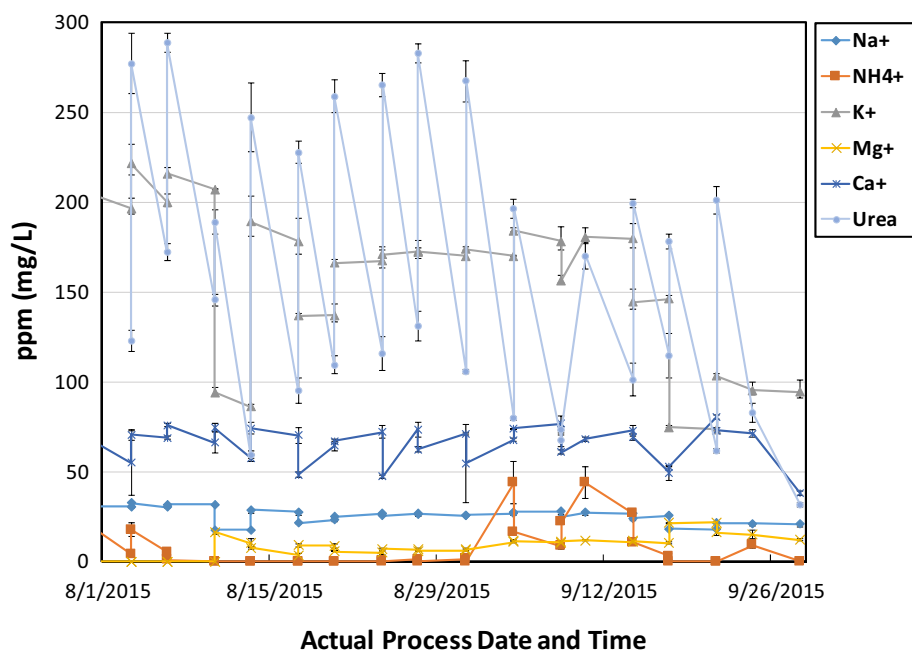
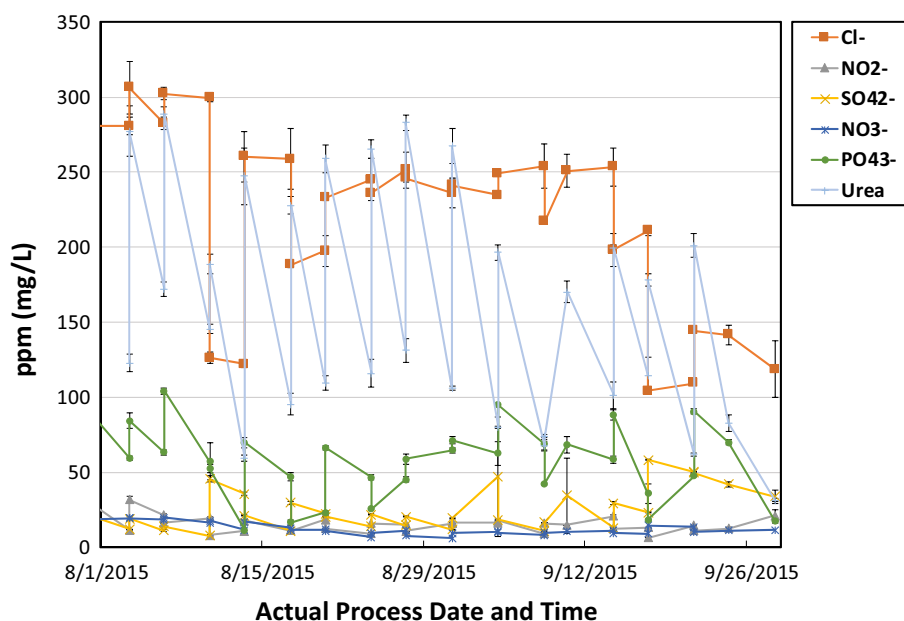


Fig. 14 Concentration of anionic species and urea in the PBR vs. time. *Error bars* represent the standard deviation of single measurements on triplicate samples. Note that the substantial decreases in Cl^- concentration on August 10 and September 14 were due to the fact that fresh make-up water was added to the reactor (after algae harvesting) instead of recycled growth medium



temperature of ca. 5 °C during this period. Interpolation of the literature data suggests that a temperature increase of 5 °C within the reactor would increase the urea hydrolysis reaction rate constant by ~25 % [25].

Another notable feature of Figs. 13 and 14 is the high concentration of K^+ and Cl^- . Given that muriate of potash (used as a nutrient) was the sole contributor of KCl to the system and that the changes in Cl^- and K^+ concentrations mirror one another, it is evident that the rather saline conditions observed in the reactor were due to overfeeding of this particular nutrient. However, this saline environment was evidently well tolerated by the algae. Also noteworthy is the rather low SO_4^{2-} concentration, which averaged 25.1 ± 13.7 ppm during the period May–September (only data for August and September are shown) with occasional spikes as high as ~50 ppm. As highlighted above, this observation is consistent with SO_4^{2-} uptake by the algae. Similarly, the concentration of NO_3^- in the system remained consistently low (with an average value of 12.1 ± 3.8 ppm), indicating that NO_x captured by the system as nitrate was utilized by the algae as a nitrogen source in addition to the added urea.

Solar shading analysis

Any endeavor to maximize PBR productivity must include efforts to optimize the exposure to—and utilization of—the available light energy by the algae culture [26]. In view of this, the effect of solar availability and self-shading on a rudimentary digital model of the cyclic flow PBR was undertaken. The software package employed, Autodesk Ecotect Analysis, is an environmental analysis tool that

allows architectural designers to simulate building performance from the earliest stages of conceptual design and includes both solar access and solar shading tools. To model the PBR, its geometry was reduced to a series of flattened two-dimensional planes. Each of these planar surfaces measured 2.75 m tall \times 6 m long and represented a bank of 72 tubes, resulting in a total volume of 1135 L for each row. A complete PBR system was composed of several rows of staggered tube banks (planar surfaces) spaced apart at a set interval of x (Fig. 15).

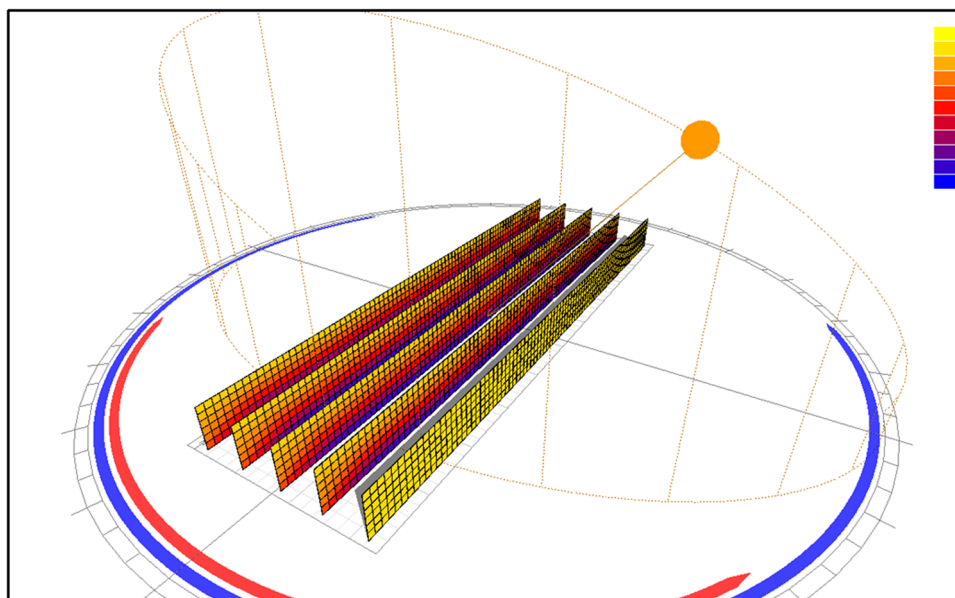
Solar orientation analysis

As anticipated, a series of initial studies showed that positioning of the PBR system with the long axis oriented along a north–south line resulted in substantially more exposure to direct sunlight, or photosynthetically active radiation (PAR), than did an orientation along an east–west line. In order for a PBR oriented in an east to west direction to receive similar amounts of direct sunlight as one oriented in a north–south direction, the spacing between rows (x) would have to be considerably larger.

Self-shading analysis

After determining the desired orientation of the PBR system, Ecotect was used to investigate the effects of self-shading on the PBR system and thus establish the value of x at which areal productivity is highest. For this analysis, three values of x (1, 1.5 and 2 m) were tested to see which produced the highest value of productivity for a given area of land measuring 30 m \times 6 m (180 m²). Using these

Fig. 15 Schematic showing PBR model used for solar shading analysis



values of x resulted in three different PBRs of varying size: when $x = 1$ m, the PBR consisted of 31 rows for a total system volume of 35,185 L; when $x = 1.5$ m, the PBR consisted of 21 rows for a total system volume of 23,835 L; and when $x = 2$ m, the PBR consisted of 16 rows for a total system volume of 18,160 L.

For each of these spacing conditions, a self-shading analysis was performed on one row of tubes in the middle of the PBR array to determine the effect of shading on the row by the two rows immediately adjacent to it. This shading analysis was performed for the date of the summer solstice (June 22, 2015), when the earth's axial tilt is most inclined towards the sun and, therefore, the sun appears at its highest point in the sky. The shading analysis diagrams for x values of 1, 1.5 and 2 m are shown in Fig. 16. These diagrams show the percentage of the (planar) PBR surface that is shaded by the adjacent rows of tubes. The blue lines running across the circle represent the path of sun in the sky, with the line for June 22 being located at the top. Within the circle, the areas shown in white represent a condition of no shading (0 %) while areas shown in black represent a condition of total shading (100 %). Similarly, the varying shades of gray represent conditions of partial shading. Therefore, the greater the amount of white-colored area in the diagram, the less self-shading the PBR experiences and the more sunlight it receives.

Unsurprisingly, these results show that the amount of self-shading decreases as the value of x increases. This finding is supported by a graph of the corresponding shading values (Fig. 17a), which shows that a spacing of 2 m results in the PBR receiving 0 % shade for ~5 h a day

versus 4 h when $x = 1.5$ m and 3 h when $x = 1$ m. However, while this provides a relatively quick means of assessing the effect of self-shading on individual rows, it does not correlate directly to predicting the effect of this shading on the overall areal productivity of the PBR system. To accomplish this, the numerical data collected from the self-shading analysis must be combined with average algal growth rates.

The data collected from the self-shading analysis consisted of a series of percentage-shaded values listed for every half-hour of the chosen day (June 22). The fraction of the PBR row that remained unshaded [1.0 minus (–) the fraction-shaded value] was multiplied by the total system volume for that particular PBR (based on the x values) to calculate the photosynthetically active volume of the reactor for that half-hour period. This volume was then multiplied by the average algal growth rate for a 30-min period—0.015 g/L, corresponding to the maximum growth rate observed at East Bend Station when growing conditions were ideal (i.e., around midday when there was no solar shading)—to obtain the total system growth for that half-hour. This calculation was done for all half-hour periods considered (8:00 a.m.–6:00 p.m.) and the resulting values were compared for all three reactors ($x = 1$ m, $x = 1.5$ m, and $x = 2$ m; see Fig. 17b). These values were then totaled for each reactor and divided by the area of land used to calculate the areal productivity of each reactor. For the reactor where $x = 1$ m, the estimated productivity was determined to be 38.6 g/(m² day) (6940 g/180 m²). Similarly, for the systems where $x = 1.5$ m and $x = 2$ m, the areal productivity was calculated to be

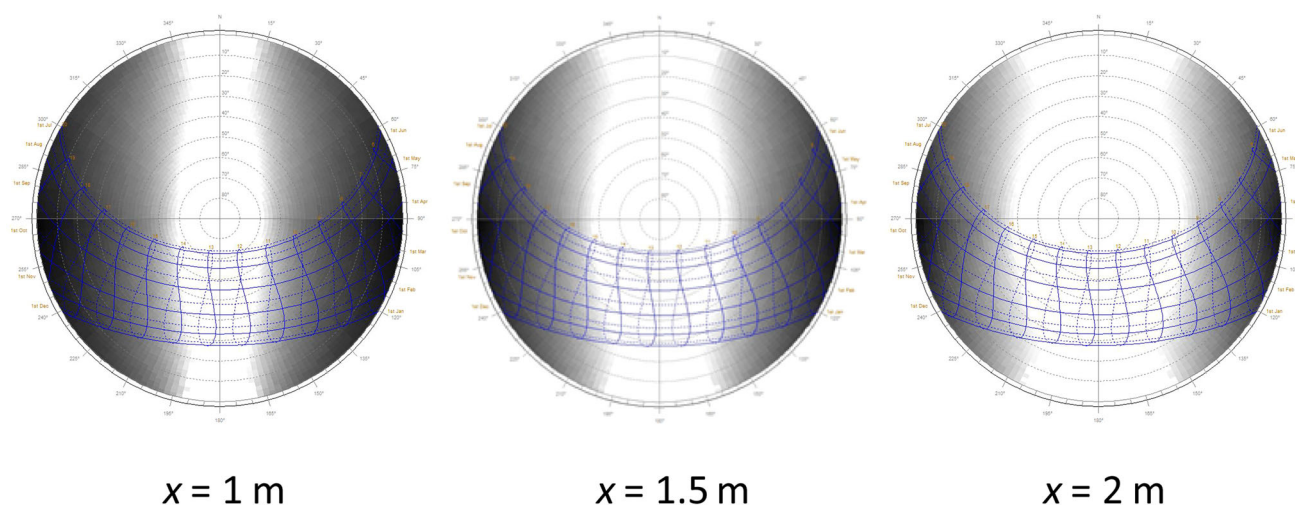


Fig. 16 Shading analysis diagrams for PBR row spacings (x) of 1, 1.5 and 2 m

32.1 and 27.0 g/(m² day), respectively. Even with the increased amount of self-shading that occurs in the reactor where $x = 1$ m, the areal productivity is higher as a result of its greater total system volume (made possible by the closer spacing of the rows) when compared with the PBRs with x values of 1.5 and 2 m. Figure 17c shows a comparison of the total algae growth (g) of each reactor shown over time for a 10-hour period. This graph shows that the total daily output of the PBR where $x = 1$ m is 143 % higher than that of the PBR where $x = 2$ m (6940 vs. 4865 g).

These studies provide a qualitative indication that closer spacing, even though it produces higher levels of self-shading, results in a significant increase in areal productivity.¹ While this approach to solar shading analysis is promising, it is important to emphasize that the accuracy of the results should not be overestimated. Several assumptions were made during this study, i.e., that algae growth occurs only within the photosynthetically active PBR volume, that light transmission through the PBR rows is negligible (a fair assumption if reasonably high culture densities are maintained), that light scattering from unshaded to shaded areas can be neglected, and that the growth rate (in g/L) is constant throughout the day. This latter assumption takes no account of the fact that growth rates during the first few hours of the day are likely to be lower than later on, due to overnight cooling of the culture. It should also be

¹ Naturally, this increased productivity comes at the cost of the increased capital expenditure associated with higher PBR tube densities. Consequently, an optimum PBR design should ultimately balance areal productivity with cost. In other words, the ultimate goal must be to identify the point at which increased areal productivity is not economically justified.

appreciated that at other times of the year, when the sun's trajectory is lower and self-shading occurs for more extended periods of time, the benefit of closer tube spacing will be less significant. However, the results of these analyses provide a starting point for more detailed calculations.

Conclusions

The results from this study reinforce our previous findings that CO₂ capture and recycle using microalgae are feasible from a technical standpoint. Using a novel cyclic flow photobioreactor and a strain of *S. acutus*, average CO₂ capture efficiency of 44 % was achieved during daylight hours in September 2015, using a flue gas sparge time of 5 s/min. The PBR at East Bend Station also served as a secondary scrubber for NO_x and SO_x, removing on average 41.5 % of the NO_x and 100 % of the SO_x from the flue gas. The PBR was successfully operated in continuous mode during the period May–September 2015, during which algae productivity of 0.165 ± 0.057 g/(L day) was obtained.

The effect of solar availability and self-shading on a rudimentary digital model of the cyclic flow PBR was examined using Autodesk Ecotect Analysis software. Initial results for June 22 (the summer solstice) showed that within the range studied (1.0–2.0 m), closer spacing of tube rows, while producing higher levels of self-shading, should result in increased areal productivity due to the increased culture volume per unit area. These findings suggest that this is a promising approach for the optimization of PBR layout with respect to the utilization of available solar radiation and provides a starting point for more detailed studies.

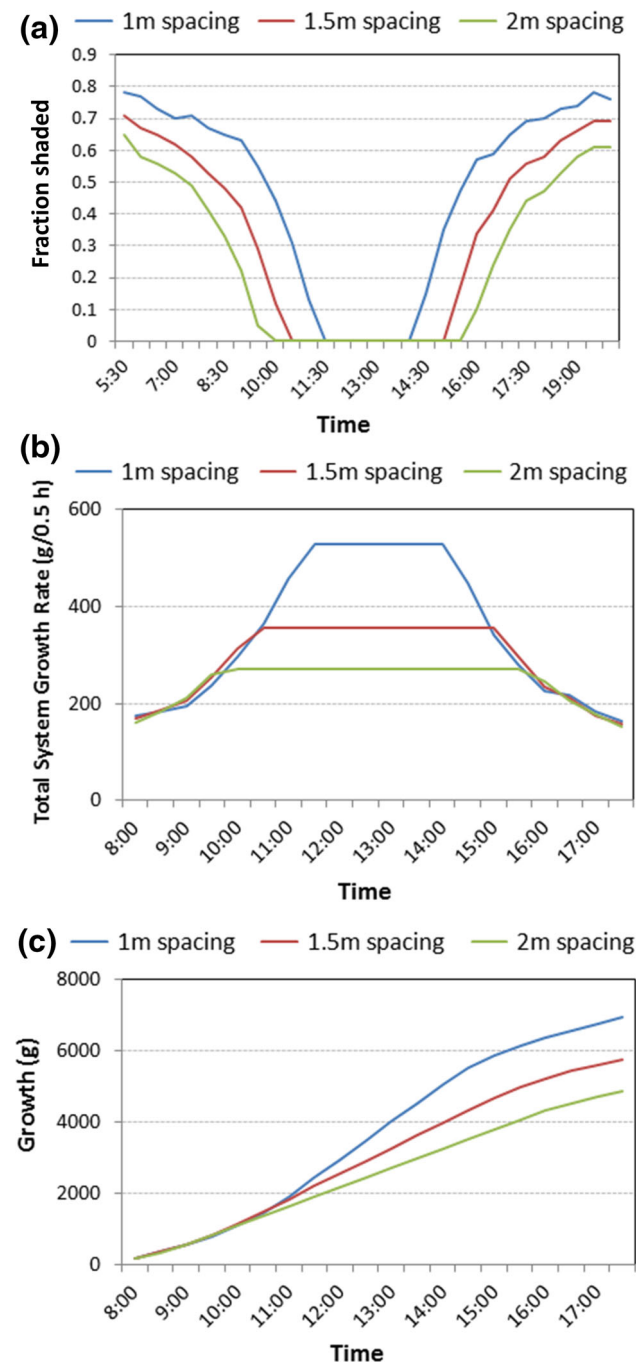


Fig. 17 Effect of PBR row spacing on **a** PBR self-shading; **b** calculated algae growth rate; **c** calculated cumulative algae growth

Acknowledgments The authors would like to thank Landon Caudill, Charles Cecil, Katelyn Yohe, Wesley Fluty, Markus Montee and Travis Jarrells for their assistance with photobioreactor construction and algae harvesting. We would also like to acknowledge the considerable assistance of Doug Durst (Duke Energy) with the activities at East Bend Station. The Kentucky Department of Energy Development and Independence, Duke Energy and the University of Kentucky are thanked for financial support.

Open Access This article is distributed under the terms of the Creative Commons Attribution 4.0 International License (<http://creativecommons.org/licenses/by/4.0/>), which permits unrestricted use, distribution, and reproduction in any medium, provided you give appropriate credit to the original author(s) and the source, provide a link to the Creative Commons license, and indicate if changes were made.

References

1. US Department of Energy (2007) Cost and performance baseline for fossil energy plants volume 1: bituminous coal and natural gas to electricity, revision 1. DOE/NETL-2007/1281
2. Laws EA, Berning JL (1991) A study of the energetics and economics of microalgal mass culture with the marine Chlorophyte *Tetraselmis suecica*: implications for use of power plant stack gases. *Biotechnol Bioeng* 37:936–947
3. Matsumoto H, Shioji N, Hamasaki A, Ikuta Y, Fukuda Y, Sato M, Endo N, Tsukamoto T (1995) Carbon dioxide fixation by microalgae photosynthesis using actual flue gas discharged from a boiler. *Appl Biochem Biotechnol* 51(52):681–692
4. Kadam KL (1997) Power plant flue gas as a source of CO₂ for microalgae cultivation: economic impact of different process options. *Energy Convers Manag* 38:S505–S510
5. Zhang X (2015) Microalgae removal of CO₂ from flue gas. IEA clean coal centre. ISBN 978-92-9029-572-3
6. Hanagata N, Takeuchi T, Fukuju Y, Barnes DJ, Karube I (1992) Tolerance of microalgae to high CO₂ and high temperature. *Phytochemistry* 31(10):3345–3348
7. Sakai N, Sakamoto Y, Kishimoto N, Chihara M, Karube I (1995) *Chlorella* strains from hot springs tolerant to high temperature and high CO₂. *Energy Convers Manag* 36:693–696
8. De Moraes MG, Costa JAV (2007) Isolation and selection of microalgae from coal fired thermoelectric power plant for biofixation of carbon dioxide. *Energy Convers Manag* 48(7):2169–2173
9. Westerhoff P, Hu Q, Esspaza-Soto Vermaas W (2010) Growth parameters of microalgae tolerant to high levels of carbon dioxide in batch and continuous-flow photobioreactors. *Environ Technol* 31:523–532
10. Negoro M, Shioji N, Miyamoto K, Miura Y (1992) Growth of microalgae in high CO₂ gas and effects of SO_x and NO_x. *Appl Biochem Biotechnol* 28–29:877–886
11. Lee JS, Kim DK, Lee JP, Park SC, Koh JH, Cho HS, Kim SW (2002) Effects of SO₂ and NO on growth of *Chlorella* sp. KR-1. *Bioresour Technol* 82(1):1–4
12. Kumar A, Ergas S, Yuan X, Sahu A, Zhang Q, Dewulf J, Malcata FX, van Langenhove H (2010) Enhanced CO₂ fixation and bio-fuel production via microalgae: recent developments and future directions. *Trends Biotechnol* 28(7):371–380
13. Murakami M, Ikenouchi M (1997) The biological CO₂ fixation and utilization project by rite (2)—screening and breeding of microalgae with high capability in fixing CO₂. *Energy Convers Manag* 38:S493–S497
14. Olaizola M (2003) Microalgal removal of CO₂ from flue gases: changes in medium pH and flue gas composition do not appear to affect the photochemical yield of microalgal cultures. *Biotechnol Bioprocess Eng* 8:360–367
15. Crofcheck C, Shea A, Montross M, Crocker M, Andrews R (2013) Influence of flue gas components on the growth rate of *Chlorella vulgaris* and *Scenedesmus acutus*. *Trans ASABE* 56(6):1421–1429

16. Wang B, Li Y, Wu N, Lan CQ (2008) CO₂ bio-mitigation using microalgae. *Appl Microbiol Biotechnol* 79:707–718
17. Seambiotic Ltd (2010) Algae pilot plant. <http://www.seambiotic.com/News/scientific-white-papers>. Accessed August 2010
18. Wilson MHW, Groppo J, Placido A, Graham S, Morton SA, Santillan-Jimenez E, Shea A, Crocker M, Crofcheck C, Andrews R (2014) CO₂ recycling using microalgae for the production of fuels. *Appl Petrochem Res* 4:41–53
19. Williams PJB, Laurens LML (2010) Microalgae as biodiesel and biomass feedstocks: review and analysis of the biochemistry, energetics and economics. *Energy Environ Sci* 3(5):554–590
20. Ugwu CU, Aoyagi H, Uchiyama H (2008) Photobioreactors for mass cultivation of algae. *Bioresour Technol* 99(10):4021–4028
21. Crofcheck C, Xinyi E, Shea A, Montross M, Crocker M, Andrews R (2012) Influence of media composition on the growth rate of *Chlorella vulgaris* and *Scenedesmus acutus* utilized for CO₂ mitigation. *J Biochem Technol* 4(2):589–594
22. Groppo J, Rhea N, Shin HY et al (2014) Microalgae processing for the production of fuels. In: 4th international conference on algal biomass, ALGA2014_0165, biofuels and bioproducts, Santa Fe
23. Green D (2008) Perry's chemical engineers' handbook, 8th edn. McGraw Hill, New York, p 2-129 (**Table 2–122**)
24. Green D (2008) Perry's chemical engineers' handbook, 8th edn. McGraw Hill, New York, pp 2-126–2-127 (**Table 2–122**)
25. Warner R (1942) The kinetics of the hydrolysis of urea and arginine. *J Biol Chem* 142:705–723
26. Benson BC, Rusch KA (2006) Investigation of light dynamics and their impact on algal growth rate in a hydraulically integrated serial turbidostat algal reactor (HISTAR). *Aquac Eng* 35:122–134